ISSN 0021-3640, JETP Letters, 2023, Vol. 118, No. 5, pp. 328–335. © The Author(s), 2023. This article is an open access publication.
Russian Text © The Author(s), 2023, published in Pis'ma v Zhurnal Eksperimental'noi i Teoreticheskoi Fiziki, 2023, Vol. 118, No. 5, pp. 330–337.

CONDENSED MATTER

Interplay between Magnetism and Topology in $MnBi_2Te_4$

V. V. Val'kov[a], *, A. O. Zlotnikov[a], and A. Gamov[a]

[a] *Kirensky Institute of Physics, Federal Research Center KSC, Siberian Branch, Russian Academy of Sciences, Krasnoyarsk, 660036 Russia*

**e-mail: vvv@iph.krasn.ru*

Received July 21, 2023; revised July 26, 2023; accepted July 28, 2023

The dependence of the topology of the fermion excitation spectrum on the magnetic state of the system is analyzed taking into account the structure of the Te–Mn–Te trilayer in the Te–Bi–Te–Mn–Te–Bi–Te layer sequence of the $MnBi_2Te_4$ van der Waals single crystal, crystal field effects, spin–orbit coupling, and the covalent mixing of electronic states of Mn^{2+} ions with electronic states of Te^{2-} ions in the strong electron correlation regime. The Chern number in the ferromagnetic phase, which is due to the kinematic interaction between Hubbard fermions, is equal to 1; i.e., the topology of the band structure of the Te–Mn–Te trilayer is nontrivial. The Chern number in the paramagnetic phase is zero; i.e., the topology is trivial. The magnetic moments of Mn^{2+} ions for the constructed spin orbitals are perpendicular to the layers. The magnetic moments of Mn^{2+} ions in the nearest layers are antiferromagnetically ordered via the Anderson mechanism.

DOI: 10.1134/S0021364023602336

1. INTRODUCTION

The formation of a long-range magnetic order in topological insulators leads to some nontrivial effects such as the formation of a band gap in the excitation spectrum of surface states and the realization of the quantum anomalous Hall effect [1–3]. A nontrivial topology of the electronic structure with the formation of bulk inverted bands and a Dirac cone corresponding to surface states at the appearance of the long-range antiferromagnetic order in $MnBi_2Te_4$ have been recently predicted in ab initio calculations [4–6] and are confirmed by angle-resolved photoemission spectroscopy [5, 7]. Thus, the $MnBi_2Te_4$ compound belongs to antiferromagnetic topological insulators described in [8].

The $MnBi_2Te_4$ compound includes a sequence of seven layers Te–Bi–Te–Mn–Te–Bi–Te (septuple layers) perpendicular to the z axis [9]. Each layer has a triangular lattice. The magnetic structure of Mn is characterized by the easy-axis anisotropy perpendicular to the layers [10]. Mn ions in a layer are ferromagnetically ordered. Inelastic neutron scattering data also demonstrate the presence of competing antiferromagnetic exchange between next neighbors in the layer with the exchange coupling constant close to the critical value at which the type of the magnetic structure changes [11]. The A-type antiferromagnetic order is formed between Mn layers with a Néel temperature of 24 K.

Despite the performed ab initio calculations of the electronic structure of $MnBi_2Te_4$, the development of the effective low-energy model allows a significant advance in the understanding and simplification of the description of topological features of the material and surface states. An effective model of Te–Bi bilayers including the contribution from the magnetic Mn ions was formulated in [4]. This model made it possible to demonstrate that surface states penetrate to a depth of two septuple layers [12].

Topological invariant is nontrivial for $MnBi_2Te_4$ films containing an odd number of septuple layers [6, 13]. Thus, compounds with an uncompensated magnetic moment near the surface of the sample are of interest. In this case, a gap appear in the Dirac cone of surface states of the antiferromagnetic topological insulator, which is due to the breaking of the symmetry with respect to the successive application of the time reversal and primitive translation operations. It is known that the band gap in different samples varies strongly from a vanishingly small value to tens of meV. Possible reasons for this variation was discussed in [14].

Despite mentioned successes in the understanding of the appearing nontrivial topology in $MnBi_2Te_4$, some problems are still unsolved. In particular, a reason for the formation of the ferromagnetic order in Mn ion layers at the insulator ground state of the compound under consideration is mysterious. An origin of the strong uniaxial anisotropy in Mn ion layers is also poorly studied. The effect of the covalent mixing of spin orbitals of Mn and Te ions on the band structure of the system and its topological properties is of a primary significance in these problems.

These problems are discussed in this work.

2. BASIS STATES OF THE Te–Mn–Te SYSTEM AND THE HAMILTONIAN OF THE TRILAYER IN THE WANNIER REPRESENTATION

Three-layer Te–Mn–Te subsystems play a significant role in the formation of the band structure with nontrivial topology in the $MnBi_2Te_4$ topological magnetic compound. They consist of a Mn^{2+} ion layer and Te^{2-} ion layers above and below it. Ions in each layer are located at the sites of a triangle lattice. The sites of Te lattices are shifted from the positions of Mn ions as shown in Fig. 1.

To construct the basis of electronic states and the Hamiltonian presenting the structure of the energy bands near the chemical potential, we take into account the splitting of electron configurations s of $3d^5$ Mn^{2+} and $5p^6$ Te^{2-} ions in the presence of the crystal field and the spin–orbit coupling.

Mn^{2+} ions are in the crystal field of the trigonal symmetry (point group $\mathbf{D}_{3d}$). Consequently, a tenfold degenerate (taking into account the spin of the electron) $3d$ level is split into a set of doublets according to the Kramers theorem.

The Wigner–Eckart theorem allows one to establish a relation between split energy levels and the form of spin orbitals in terms of the equivalent Hamiltonian. This Hamiltonian for the group $\mathbf{D}_{3d}$ has the form [15]

$$H_0 = B_2^0\hat{O}_2^0 + B_4^0\hat{O}_4^0 + B_4^3\hat{O}_4^3 - \lambda(\mathbf{Ls}), \qquad (1)$$

where B_n^m are the parameters of the crystal field, $\hat{O}_n^m$ are the Stewens operators [16], λ is the spin–orbit coupling constant, and $\mathbf{L}$ and s are the orbital angular momentum and spin operators of the electron, respectively.

Since the main splitting effects are due to the octahedral components of the crystal field, most of the states of the equivalent Hamiltonian still allows the classification in the projection of the orbital angular momentum and spin.

Under the conditions

$$5B_4^0 < B_2^0 < -(20/3)B_4^0, \quad B_4^0 < 0, \qquad (2)$$

a situation occurs, where a half-filled doublet corresponds to the spin orbitals $|\Psi_{f\sigma}^{(d)}\rangle$ [17]

$$\begin{aligned}|\Psi_{f\uparrow}^{(d)}\rangle &= a|f;+2\uparrow\rangle + b|f;-1\uparrow\rangle + c|f;0\downarrow\rangle,\\ |\Psi_{f\downarrow}^{(d)}\rangle &= a|f;-2\downarrow\rangle - b|f;+1\downarrow\rangle - c|f;0\uparrow\rangle.\end{aligned} \qquad (3)$$

Here, $|a| \gg |b|, |c|$. In this case, two other doublets completely filled with electrons have lower energies and become insignificant for a further consideration. The remaining two doublets have much higher energies and can be neglected.

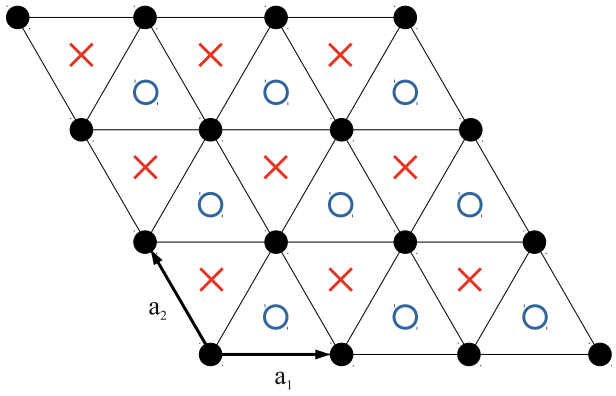

Fig. 1. (Color online) Fragment of the crystal structure of the Te–Mn–Te trilayer. The Te^{2-} ions, which are ordered according to a triangular lattice, are located above and below the Mn^{2+} ions, which are marked by filled circles and form a triangular lattice in the middle plane of the trilayer. The red crosses and empty circles mark the projections of the upper and lower Te^{2-} ions on the middle plane of the trilayer, respectively.

Here and below, it is assumed that Mn^{2+} ions are located at sites that are specified by the Latin letters f, f',... and form an F sublattice. The right-hand sides of Eqs. (3) are the superpositions of states each denoted by a ket vector specified by the site number f, the projection of the orbital angular momentum of the d state, and the spin projection. The parameters of the equivalent Hamiltonian used in the calculations were $B_2^0 = 0.3$, $B_4^0 = -0.2$, $B_4^3 = 0.1$, $\lambda = -0.2$.

The spin orbitals $|\Psi_{f\sigma}^{(d)}\rangle$ are important because they constitute basis functions forming an itinerant band, which is related to $3d$ Mn ion states and is located near the chemical potential. The prevailing contribution to the spin orbitals from states with the largest magnitude of the projection of the total angular momentum $J_z = L_z + s_z$ is significant for the further consideration.

In this basis, the Hamiltonian H_d of the subsystem of electronic states on Mn^{2+} ions can be written in the tight-binding scheme in the form

$$\hat{H}_d = \sum_f [\varepsilon_d\hat{n}_f + U\hat{n}_{f\uparrow}\hat{n}_{f\downarrow}] + \sum_{ff'\sigma} t_{ff'}^d d_{f\sigma}^+ d_{f'\sigma}. \qquad (4)$$

Here, the summation over the indices f and f' corresponds to the summation over the sites of the lattice that are occupied with Mn ions, ε_d is the energy of the electron on the Mn^{2+} ion, $d_{f\sigma}^+(d_{f\sigma})$ are the Fermi operators used to describe the creation (annihilation) of an electron with the spin projection $\sigma = \pm 1/2$ at the fth site, $\hat{n}_{f\sigma} = d_{f\sigma}^+ d_{f\sigma}$ is the electron number operator at the fth site with the spin projection σ, U is the Hub-

bard repulsion energy, and $t^d_{ff'}$ is the electron hopping integral between Mn ions at the fth and f'th sites. It is seen that the operator $\hat{H}_d$ given by Eq. (4) is the Hamiltonian of the Hubbard model [18] for the triangular lattice.

The positions of Te^{2-} ions located above and below the Mn ion layer (they are marked by red crosses and blue circles in Fig. 1, respectively) are specified by the indices g, g',...and l, l',..., respectively.

The spin orbitals $|\Psi^{(p)}_{g\sigma}\rangle$ and $|\Psi^{(p)}_{l\sigma}\rangle$ appearing after the splitting of the $5p^6$ terms of Te^{2-} ions at the gth and lth sites in the trigonal symmetry field (point group $\mathbf{C}_{3v}$) and in the presence of the spin–orbit coupling, as in the Bernevig–Hughes–Zhang (BHZ) model [19–22], are represented in the form

$$\begin{aligned} |\Psi^{(p)}_{g\uparrow}\rangle &= |g;1\uparrow\rangle,\ |\Psi^{(p)}_{g\downarrow}\rangle = |g;-1\downarrow\rangle,\\ |\Psi^{(p)}_{l\uparrow}\rangle &= |l;1\uparrow\rangle,\ |\Psi^{(p)}_{l\downarrow}\rangle = |l;-1\downarrow\rangle. \end{aligned} \tag{5}$$

Here, the ket vectors on the right-hands sides are the p-wave function at the gth and lth sites with given projections of the orbital angular momentum ±1 and the spin.

Since the spin orbitals of Te^{2-} ions form two subsystems of p electron states, the Hamiltonian H_p for them can be represented in the form

$$\begin{aligned} \hat{H}_p &= \sum_{g\sigma}\varepsilon_p p^+_{1g\sigma}p_{1g\sigma} + \sum_{l\sigma}\varepsilon_p p^+_{2l\sigma}p_{2l\sigma}\\ &+ \sum_{gg'\sigma}t^p_{gg'}p^+_{1g\sigma}p_{1g'\sigma} + \sum_{ll'\sigma}t^p_{ll'}p^+_{2l\sigma}p_{2l'\sigma}\\ &+ \sum_{gl\sigma}\{t^p_{gl}p^+_{1g\sigma}p_{2l\sigma} + \text{H.c.}\}. \end{aligned} \tag{6}$$

Here, the summation over the indices g and l means the summation over Te ions at sites above and below the Mn ion plane, respectively; ε_p is the energy of the p electron on the Te^{2-} ion; $p^+_{1g\sigma}(p_{1g\sigma})$ is the creation (annihilation) operator of the p electron with the spin projection $\sigma = \pm1/2$ on the Te ion at the gth site above the Mn ion plane; a similar notation with the index l instead of g is used for the creation (annihilation) operator of the p electron with the spin projection $\sigma = \pm1/2$ on the Te ion at the lth site below the Mn ion plane; $t^p_{gg'}$ ($t^p_{ll'}$) are the p electron hopping integral between Te ions at the gth and g'th sites (the lth and l'th sites) located above (below) the Mn ion plane; and t^p_{gl} is the p electron hopping integral between Te ions at the gth and lth sites located above and below the Mn ion plane, respectively.

The covalent mixing (hybridization) of spin orbitals of Te^{2-} and Mn^{2+} ions makes important contribution to the formation of the band structure with nontrivial topology in the considered system. The intensity of this mixing is determined by the electron hopping integral between these groups of states. In this case, the dependence of this hopping integral on the hopping direction is of more significance than the magnitude of this integral.

The covalent mixing operator with allowance for p–d hybridization only between the nearest Mn^{2+} and Te^{2-} ions has the form

$$\begin{aligned} \hat{T}_{pd} &= \sum_{f\delta\sigma}\{t^\sigma_{pd}(\delta)d^+_{f\sigma}p_{1f+\delta\sigma} + \text{H.c.}\}\\ &+ \sum_{f\gamma\sigma}\{t^\sigma_{pd}(\gamma)d^+_{f\sigma}p_{2f+\gamma\sigma} + \text{H.c.}\}. \end{aligned} \tag{7}$$

Here, δ and γ are the vectors connecting Mn ions with the nearest Te ions in the upper and lower planes of the considered trilayer, respectively.

The hybridization parameters are the matrix elements of the kinetic energy operator $\hat{T}$:

$$t^\sigma_{pd}(\delta) = \langle\Psi^{(d)}_{f\sigma}|\hat{T}|\Psi^{(p)}_{f+\delta,\sigma}\rangle, \tag{8}$$

$$t^\sigma_{pd}(\gamma) = \langle\Psi^{(d)}_{f\sigma}|\hat{T}|\Psi^{(p)}_{f+\gamma,\sigma}\rangle. \tag{9}$$

Calculations show that their dependence on the vectors δ and γ has the form

$$t^\sigma_{pd}(\delta) = t_{pd}\begin{cases}(1 - i\eta_\sigma\sqrt{3})/2, & \delta = (\mathbf{a}_1 - \mathbf{a}_2)/3,\\ -1, & \delta = (\mathbf{a}_1 + 2\mathbf{a}_2)/3,\\ (1 + i\eta_\sigma\sqrt{3})/2, & \delta = -(2\mathbf{a}_1 + \mathbf{a}_2)/3,\end{cases} \tag{10}$$

$$t^\sigma_{pd}(\gamma) = t_{pd}\begin{cases}-(1 + i\eta_\sigma\sqrt{3})/2, & \gamma = (2\mathbf{a}_1 + \mathbf{a}_2)/3,\\ 1, & \gamma = -(\mathbf{a}_1 + 2\mathbf{a}_2)/3,\\ -(1 - i\eta_\sigma\sqrt{3})/2, & \gamma = (\mathbf{a}_2 - \mathbf{a}_1)/3.\end{cases} \tag{11}$$

Here, $\mathbf{a}_1$ and $\mathbf{a}_2$ are the elementary translation vectors shown in Fig. 1.

In addition to the covalent mixing of the p and d states, the exchange between these fermions is significant:

$$\begin{aligned} \hat{J}_{pd} &= -\sum_{f\delta\sigma}Jp^+_{1f+\delta\sigma}\left(\mathbf{S}_f\boldsymbol{\tau}_{\sigma\sigma'}\right)p_{1f+\delta\sigma'}\\ &- \sum_{f\gamma\sigma}Jp^+_{2f+\gamma\sigma}\left(\mathbf{S}_f\boldsymbol{\tau}_{\sigma\sigma'}\right)p_{2f+\gamma\sigma'}. \end{aligned} \tag{12}$$

Here, J is the exchange coupling constant, $\boldsymbol{\tau}_{\sigma\sigma'} = (\tau^x_{\sigma\sigma'}, \tau^y_{\sigma\sigma'}, \tau^z_{\sigma\sigma'})$ is the vector where the components are the matrix elements of the Pauli matrices, and $\mathbf{S}_f$ is the quasispin vector operator whose components are given by the expressions

$$\begin{aligned} S^x_f = (X^{\uparrow\downarrow}_f + X^{\downarrow\uparrow}_f)/2,\quad S^y_f = (X^{\uparrow\downarrow}_f - X^{\downarrow\uparrow}_f)/(2i),\\ S^z_f = (X^{\uparrow\uparrow}_f - X^{\downarrow\downarrow}_f)/2, \end{aligned} \tag{13}$$

where X_f^{nm} are the Hubbard operators [23–25] describing transitions of ions at the fth site from the $|f,m\rangle$ to the $|f,n\rangle$ state.

Summarizing, the Hamiltonian of the Te–Mn–Te trilayer is obtained in the form

$$\hat{H} = \hat{H}_d + \hat{H}_p + \hat{T}_{pd} + \hat{J}_{pd}. \quad (14)$$

3. ENERGY STRUCTURE OF THE Te–Mn–Te TRILAYER

To determine the spectrum of fermion states of the Te–Mn–Te trilayer and to calculate the topological index of the resulting band structure, we take into account the following known properties of $MnBi_2Te_4$ affecting the choice of relations between the parameters of the Hamiltonian (14).

(i) The magnetic moments of Mn^{2+} ions in one layer at low temperatures are ferromagnetically ordered and are opposite to the magnetic moments of Mn^{2+} ions in the neighboring layers.

(ii) Frustrated exchange couplings close to the critical magnitude [11] exist between Mn ions that are located in one layer and are not the nearest neighbors.

(iii) The ground state of $MnBi_2Te_4$ is insulating although the number of electrons in the $3d^5$ electronic configuration of Mn ions is odd.

The ferromagnetic coupling between the nearest Mn^{2+} ions in one layer could be explained with the direct Heisenberg exchange, but property (ii) cannot be explained by this mechanism. The conventional band approach can hardly reproduce property (iii).

In view of the mentioned problems, we used an approach implying the presence of strong electron correlations in the subsystems of Mn ions based on the following foundations.

(i) The exact result obtained by Nagaoka [26] that the ground state of the system with one hole (and $N_e = N - 1$ electrons) in the Hubbard model in the limit $U \to \infty$ is ferromagnetic.

(ii) Since the concentration in the Te–Mn–Te trilayer is $n_d \simeq 1$, the ferromagnetic state in the layer of Mn^{2+} ions corresponds to the regime of strong electron correlations $U \gg |t_{ff'}^d|$. In this case, the formation of frustrated couplings is quite natural because an antiferromagnetic coupling appears in the second order of the perturbation theory in the parameter $|t_{ff'}^d|/U$ via the Anderson mechanism.

(iii) The ab initio calculations [5, 6] of the electronic structure of $MnBi_2Te_4$ give the values $U \simeq (4–5)$ eV for the Hubbard repulsion parameter between electrons in Mn ions.

Taking into account the electron–hole symmetry of the Hubbard Hamiltonian $\hat{H}_d$, we use the hole representation. Since the hole concentration n_d in the d subsystem per cell is no more than 1, only the lower subband of Hubbard fermions can be taken into account in the regime of strong electron correlations where $U \gg |t_{ff'}^d|$ [27–29].

The states of the upper Hubbard subband have a high energy and are insignificantly filled. Virtual transitions to these states can be taken into account in the perturbation theory in the small parameters $|t_{ff'}^d|/U \ll 1$ and $|t_{pd}|/U \ll 1$. Below, we determine the spectrum of excitations and the ferromagnetic state of the magnetic moments of Mn ions disregarding these processes.

In the quasimomentum representation

$$p_{1f+\delta\sigma} = \frac{1}{\sqrt{N}}\sum_k e^{ik(f+\delta)} p_{1k\sigma}, \quad (15)$$

$$p_{2f+\gamma\sigma} = \frac{1}{\sqrt{N}}\sum_k e^{ik(f+\gamma)} p_{2k\sigma}, \quad (16)$$

$$X_f^{0\sigma} = \frac{1}{\sqrt{N}}\sum_k e^{ikf} X_{k\sigma}, \quad (17)$$

we obtain

$$\begin{aligned}
\hat{H}_d &= \sum_{k\sigma}(\varepsilon_d + t_{dk}) X_{k\sigma}^+ X_{k\sigma},\\
\hat{H}_p &= \sum_{k\sigma}[\varepsilon_p(k)(p_{1k\sigma}^+ p_{1k\sigma} + p_{2k\sigma}^+ p_{2k\sigma})]\\
&\quad - \sum_{k\sigma}[t_{12}(k) p_{1k\sigma}^+ p_{2k\sigma} + \text{H.c.}],\\
\hat{T}_{pd} &= -\sum_{k\sigma}(t_{1k\sigma} X_{k\sigma}^+ p_{1k\sigma} + t_{2k\sigma} X_{k\sigma}^+ p_{2k\sigma} + \text{H.c.}),\\
\hat{J}_{pd} &= -\frac{3J}{N}\sum_{\lambda=1}^{2}\sum_{fkq\sigma\sigma'} e^{if(q-k)} p_{\lambda k\sigma}^+ (\mathbf{S}_f \boldsymbol{\tau}_{\sigma\sigma'}) p_{\lambda q\sigma'},
\end{aligned} \quad (18)$$

where

$$\begin{aligned}
t_{dk} &= 6t_d\gamma_{1k}, \quad \varepsilon_p(k) = -\varepsilon_p - 6t_p\gamma_{1k},\\
\gamma_{1k} &= \{\cos k_1 + \cos k_2 + \cos(k_1 + k_2)\}/3,\\
t_{12}(k) &= t_{12}\{\varphi_{1k} + \varphi_{2k} + \varphi_{3k}\},\\
t_{1k\sigma} &= t_{pd}\left\{r_\sigma\varphi_{1k} - \varphi_{2k} + r_\sigma^*\varphi_{3k}\right\}, t_{2k\sigma} = -t_{1k\bar{\sigma}}^*,\\
\varphi_{1k} &= \exp[i(k_1 - k_2)/3], \quad \varphi_{2k} = \exp[i(k_1 + 2k_2)/3],\\
\varphi_{3k} &= \exp[-i(2k_1 + k_2)/3], \quad r_\sigma = (1 - i\eta_\sigma\sqrt{3})/2.
\end{aligned} \quad (19)$$

Here, t_d and t_p are the electron hopping integrals between the spin orbitals of the nearest Mn^{2+} and Te^{2-} ions in one layer of the triangular lattice, respectively.

An important feature of the Fourier transforms of p–d hybridization hopping integrals $t_{1k\sigma}$ and $t_{2k\sigma}$ is that the spin variable affects the character of their quasimomentum dependence. In the presence of the overlapping of the lower d hole subband with the p sub-

band, this feature leads to an odd Chern number for the band structure and to nontrivial topology in the presence of ferromagnetic order.

The quasimomentum dependence of the electron hopping integrals between the nearest spin orbitals of Te^{2-} ions from different layers in the Te–Mn–Te trilayer is described by the quasimomentum dependence of the amplitude of the corresponding process $t_{12}(k)$.

To calculate the band structure of the trilayer, to derive self-consistent equations, and to determine the topological properties of the band structure, we introduce the three-component field operator

$$\hat{\Psi}^+_{k\sigma} = \left(p^+_{1k\sigma},\ X^+_{k\sigma},\ p^+_{2k\sigma}\right) \tag{20}$$

and define the two-time retarded matrix Green's function $\hat{D}_{k\sigma}(\omega)$ [30, 31] in terms of the Fourier transform

$$\langle\langle \hat{\Psi}_{k\sigma}(t) | \hat{\Psi}^+_{k\sigma}(t')\rangle\rangle = \int \frac{d\omega}{2\pi} e^{-i\omega(t-t')} \hat{D}_{k\sigma}(\omega). \tag{21}$$

The field operators $\hat{\Psi}_{k\sigma}$ and $\hat{\Psi}^+_{k\sigma}$ are taken in the Heisenberg representations at the times t and t', respectively.

Using the Zwanzig–Mori projection method [32, 33], we obtain the following equation for the Green's function:

$$\left[\omega\hat{I} - \hat{M}_\sigma(k)\right]\hat{D}_{k\sigma}(\omega) = \hat{P}_\sigma. \tag{22}$$

Here, $\hat{I}$ is the identity matrix; $\hat{P}_\sigma$ is the diagonal matrix with the elements $(1, N_{0\sigma}, 1)$, where $N_{0\sigma} = \langle X^{00}_f + X^{\sigma\sigma}_f\rangle$; and

$$\hat{M}_\sigma(k) = \begin{pmatrix} \varepsilon_{p\sigma}(k) & -t^*_{1k\sigma} & -t_{12}(k) \\ -N_{0\sigma}t_{1k\sigma} & \varepsilon_{dk\sigma} & -N_{0\sigma}t_{2k\sigma} \\ -t^*_{12}(k) & -t^*_{2k\sigma} & \varepsilon_{p\sigma}(k) \end{pmatrix}, \tag{23}$$

where $\varepsilon_{p\sigma}(k) = \varepsilon_p(k) - 2J_0M\sigma$, $J_0 = 3J$, $\sigma = \pm 1/2$, $M = \langle S^z_f\rangle$, and

$$\varepsilon_{dk\sigma} = \varepsilon_d + N_{0\sigma}t_{dk} - \frac{1}{N_{0\sigma}N}\sum\nolimits_q t_q \langle X^+_{q\bar{\sigma}} X_{q\bar{\sigma}}\rangle \tag{24}$$

is the energy of Hubbard fermions in the d subsystem renormalized by the kinematic interaction.

Equation (22) gives three spectral branches

$$\begin{aligned} E_{1k\sigma} &= -W_{k\sigma}/2 - \lambda_{k\sigma} - a_{k\sigma}/3, \\ E_{2k\sigma} &= -W_{k\sigma}/2 + \lambda_{k\sigma} - a_{k\sigma}/3, \\ E_{3k\sigma} &= W_{k\sigma} - a_{k\sigma}/3. \end{aligned} \tag{25}$$

Here,

$$\begin{aligned} W_{k\sigma} &= Z_{k\sigma} - P_{k\sigma}/Z_{k\sigma}, \\ Z_{k\sigma} &= \left(\sqrt{Q^2_{k\sigma} + P^3_{k\sigma}} - Q_{k\sigma}\right)^{1/3}, \end{aligned} \tag{26}$$

$$\lambda_{k\sigma} = \sqrt{-3P_{k\sigma} - 3W^2_{k\sigma}/4}$$

are functions of the quasimomentum and the spin projection and are related to the initial energy parameters as

$$\begin{aligned} P_{k\sigma} &= (b_{k\sigma} - a^2_{k\sigma}/3)/3, \\ Q_{k\sigma} &= (c_{k\sigma} + 2a^3_{k\sigma}/27 - a_{k\sigma}b_{k\sigma}/3)/2, \\ a_{k\sigma} &= -(2\varepsilon_{p\sigma}(k) + \varepsilon_{dk\sigma}), \quad b_{k\sigma} = 2\varepsilon_{p\sigma}(k)\varepsilon_{dk\sigma} \\ &\quad + \varepsilon^2_{p\sigma}(k) - |t_{12}(k)|^2 - N_{0\sigma}(|t_{1k\sigma}|^2 + |t_{2k\sigma}|^2), \\ c_{k\sigma} &= -\varepsilon^2_{p\sigma}(k)\varepsilon_{dk\sigma} + N_{0\sigma}\left[t_{12}(k)t_{1k\sigma}t^*_{2k\sigma} + \text{H.c.}\right] \\ &\quad + \varepsilon_{dk\sigma}|t_{12}(k)|^2 + \varepsilon_{p\sigma}(k)N_{0\sigma}\left(|t_{1k\sigma}|^2 + |t_{2k\sigma}|^2\right). \end{aligned} \tag{27}$$

To close the self-consistent equations, we used the components of the Green's function determined from Eq. (22):

$$\begin{aligned} D^\sigma_{11}(k,\omega) &= \frac{(\omega - \varepsilon_{dk\sigma})(\omega - \varepsilon_{pk\sigma}) - N_{0\sigma}|t_{2k\sigma}|^2}{\det^\sigma_3(k,\omega)}, \\ D^\sigma_{22}(k,\omega) &= N_{0\sigma}\frac{(\omega - \varepsilon_{pk\sigma})^2 - |t_{12}(k)|^2}{\det^\sigma_3(k,\omega)}, \\ D^\sigma_{33}(k,\omega) &= D^\sigma_{11}(k,\omega), \end{aligned} \tag{28}$$

where $\det^\sigma_3(k,\omega)$ is the third-order determinant of the matrix $[\omega\hat{I} - \hat{M}_\sigma(k)]$.

Using these functions and the spectral theorem, we obtain the necessary expressions for average values in the form

$$N_\sigma = \langle X^{\sigma\sigma}_f\rangle = \frac{N_{0\sigma}}{N}\sum_q \frac{(E_{1q\sigma} - \varepsilon_{pq\sigma})^2 - |t_{12}(q)|^2}{\lambda_{q\sigma}(3W_{q\sigma} + 2\lambda_{q\sigma})},$$

$$N_{p\sigma} = \frac{2}{N}\sum_q \frac{(E_{1q\sigma} - \varepsilon_{dq\sigma})(E_{1q\sigma} - \varepsilon_{pq\sigma}) - N_{0\sigma}|t_{2q\sigma}|^2}{\lambda_{q\sigma}(3W_{q\sigma} + 2\lambda_{q\sigma})},$$

where $N_{p\sigma}$ is the site hole density with the spin projection σ in the p subsystem and $n_d = N_\uparrow + N_\downarrow$ is the total density of Hubbard fermions per site.

The derived equations allow one to analyze the ferro- and paramagnetic phases and to reveal a change in the topology of the band structure at the change in the magnetic state of the system.

4. TOPOLOGICAL INDEX OF THE BAND STRUCTURE OF FERMION STATES IN THE Te–Mn–Te TRILAYER

The topological index (Chern number) is defined by the expression

$$Q = -\frac{1}{2\pi}\int_{-\pi}^{\pi} dk_1 \int_{-\pi}^{\pi} dk_2 B(k), \tag{29}$$

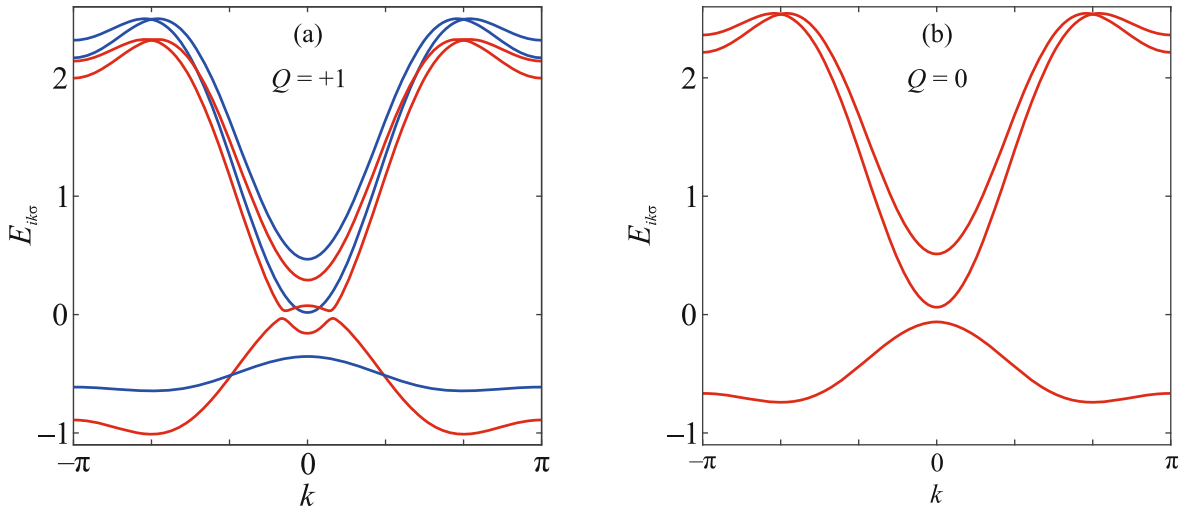

Fig. 2. (Color online) Fermion excitation spectrum for (a) unsaturated ferromagnetism for spectral branches with σ = (red lines) +1/2 and (blue lines) −1/2 and (b) paramagnetic phase, where branches are degenerate in the spin projection, according to the calculations with the parameters $t_p = 0.25$, $t_d = 0.15$, $t_{pd} = 0.05$, $J = 0.1$, $t_{12} = 0.075$, and the parameter determining the overlap of the bare d and p bands $\Delta_0 = 0.1$. In this case, $n_d = 0.97$ and $M = 0.28$. The Chern number for the ferromagnetic phase is $Q = 1$ (the topology of the band structure is nontrivial) and $Q = 0$ for the paramagnetic phase (the topology of the band structure is trivial).

where

$$B(k) = \frac{\partial A_2(k)}{\partial k_1} - \frac{\partial A_1(k)}{\partial k_2} \tag{30}$$

is the Berry curvature, which is determined as the quasimomentum derivatives of the quantities $A_1(k)$ and $A_2(k)$ obtained by averaging the operators $-i\partial/\partial k_1$ and $-i\partial/\partial k_2$ over the Bloch state [34]:

$$A_{1(2)}(k) = -i\left\langle \psi_k \left| \frac{\partial}{\partial k_{1(2)}} \right| \psi_k \right\rangle. \tag{31}$$

To establish the relation of the Berry curvature to the energy parameters, we determined the eigenvectors

$$\mathbf{R}_{k\sigma} \equiv (u_{k\sigma}, v_{k\sigma}, z_{k\sigma}) \tag{32}$$

(see, e.g., [35, 36]) of the matrix $\hat{M}_\sigma(k)$ given by Eq. (23):

$$\hat{M}_\sigma(k)\mathbf{R}_{k\sigma} = E_{k\sigma}\mathbf{R}_{k\sigma}. \tag{33}$$

After simple algebra, we obtain the Berry curvature corresponding to the lower filled band in the form

$$B_\sigma(k) = i\left[\frac{\partial v^*_{k\sigma}}{\partial k_2}\frac{\partial v_{k\sigma}}{\partial k_1} - \frac{\partial v^*_{k\sigma}}{\partial k_1}\frac{\partial v_{k\sigma}}{\partial k_2}\right] + i\left[\frac{\partial z^*_{k\sigma}}{\partial k_2}\frac{\partial z_{k\sigma}}{\partial k_1} - \frac{\partial z^*_{k\sigma}}{\partial k_1}\frac{\partial z_{k\sigma}}{\partial k_2}\right], \tag{34}$$

where

$$v_{k\sigma} = \frac{\Phi_{k\sigma}}{\sqrt{1 + |\Phi_{k\sigma}|^2 + |\Psi_{k\sigma}|^2}}, \quad z_{k\sigma} = \frac{\Psi_{k\sigma}}{\sqrt{1 + |\Phi_{k\sigma}|^2 + |\Psi_{k\sigma}|^2}}. \tag{35}$$

Here,

$$\Phi_{k\sigma} = N_{0\sigma}\frac{t^*_{12}(k)t_{2k\sigma} - t_{1k\sigma}(E_{1k\sigma} - \varepsilon_{dk\sigma})}{D_{1k\sigma}}, \tag{36}$$

$$\Psi_{k\sigma} = \frac{N_{0\sigma}t_{1k\sigma}t^*_{2k\sigma} - t^*_{12}(k)(E_{1k\sigma} - \varepsilon_{dk\sigma})}{D_{1k\sigma}}, \tag{37}$$

$$D_{k\sigma} = (E_{1k\sigma} - \varepsilon_{dk\sigma})[E_{1k\sigma} - \varepsilon_{p\sigma}(k)] - N_{0\sigma}|t_{2k\sigma}|^2. \tag{38}$$

The derived expressions show that the topology of the fermion band structure in the ferro- and paramagnetic phases is nontrivial ($Q = 1$) and trivial ($Q = 0$), respectively.

This result demonstrated in Fig. 2 indicates an intimate interplay between magnetism and topology in $MnBi_2Te_4$.

5. CONCLUSIONS

It has been shown that the covalent mixing of the p and d spin orbitals of Mn^{2+} and Te^{2-} ions in Te–Mn–Te trilayers in the van der Waals $MnBi_2Te_4$ compound is of fundamental importance for the formation of the band structure with nontrivial topology in the pres-

ence of a long-range magnetic order under the following conditions.

(i) The joint effect of the crystal field and spin–orbit coupling leads to the hierarchy of Kramers doublets of the split $3d^5$ electron configurations of Mn^{2+} ions such that a half-filled spin–orbit doublet is characterized by the parameters $\overline{L}_z \simeq 2$, $\overline{s}_z \simeq 1/2$ and $\overline{L}_z \simeq -2$, $\overline{s}_z \simeq -1/2$.

(ii) The upper spin–orbit doublets formed from the $5p^6$ electron configurations of Te^{2-} ions under the effect of the mentioned interactions, as in the BHZ model, correspond to the $|1\uparrow\rangle$ and $|-1\downarrow\rangle$ states.

(iii) The Coulomb repulsion between electrons in Mn ions is strong enough to implement the regime of strong electron correlations. In this case, the ferromagnetic state is formed in the Mn ion layer due to the kinematic interaction between Hubbard fermions [37] and induces the splitting of spin p subbands. This promotes the implementation of conditions for the overlapping of the upper energy subband of Hubbard fermions with p subbands of fermions coupled to spin orbitals of Te^{2-} ions. The Chern number in this case is +1, which corresponds to the band structure with nontrivial topology.

(iv) In the paramagnetic phase, the overlapping of bands disappears and the topology of the band structure becomes trivial. This behavior indicates the relation between the ferromagnetic ordering of the magnetic moments in the Mn ion layer to the topology of the band structure of Te–Mn–Te.

We emphasize that the magnetic moments of these ions in the ordered phase are perpendicular to the layers according to the character of the spin orbitals of Mn ions. In this case, the anisotropy is strong and results in the Ising-like behavior of the magnetic Mn ion layer. In this case, hoppings of fermions between the indicated layers lead to the antiferromagnetic coupling between the magnetic moments from different layers via the Anderson mechanism. The described picture is in complete agreement with the experimental data.

FUNDING

This work was supported by the Russian Science Foundation (project no. 23-22-10021, https://rscf.ru/project/23-22-10021/) and by the Krasnoyarsk Regional Fund of Science.

CONFLICT OF INTEREST

The authors declare that they have no conflicts of interest.

OPEN ACCESS

REFERENCES

1. R. Yu, W. Zhang, H.-J. Zhang, S.-C. Zhang, X. Dai, and Z. Fang, Science (Washington, DC, U. S.) **329**, 61 (2010).
2. X.-L. Qi and S.-C. Zhang, Rev. Mod. Phys. **83**, 1057 (2011).
3. C.-Z. Chang, J. Zhang, X. Feng, et al., Science (Washington, DC, U. S.) **340**, 167 (2013).
4. D. Zhang, M. Shi, T. Zhu, D. Xing, H. Zhang, and J. Wang, Phys. Rev. Lett. **122**, 206401 (2019).
5. M. M. Otrokov, I. I. Klimovskikh, H. Bentmann, et al., Nature (London, U.K.) **576**, 416 (2019).
6. J. Li, Y. Li, S. Du, Z. Wang, B.-L. Gu, S.-C. Zhang, K. He, W. Duan, and Y. Xu, Sci. Adv. **5**, eaaw5685 (2019).
7. Y. Gong, J. Guo, J. Li, et al., Chin. Phys. Lett. **36**, 076801 (2019).
8. R. S. K. Mong, A. M. Essin, and J. E. Moore, Phys. Rev. B **81**, 245209 (2010).
9. D. S. Lee, T.-H. Kim, C.-H. Park, C.-Y. Chung, Y. S. Lim, W.-S. Seo, and H.-H. Park, CrystEngComm. **15**, 5532 (2013).
10. Y. Li, Z. Jiang, J. Li, S. Xu, and W. Duan, Phys. Rev. B **100**, 134438 (2019).
11. B. Li, J.-Q. Yan, D. M. Pajerowski, E. Gordon, A.-M. Nedi, Y. Sizyuk, L. Ke, P. P. Orth, D. Vaknin, and R. J. McQueeney, Phys. Rev. Lett. **124**, 167204 (2020).
12. H.-P. Sun, C. M. Wang, S.-B. Zhang, R. Chen, Y. Zhao, C. Liu, Q. Liu, C. Chen, H.-Z. Lu, and X. C. Xie, Phys. Rev. B **102**, 241406 (2020).
13. M. M. Otrokov, I. P. Rusinov, M. Blanco-Rey, M. Hoffmann, A. Yu. Vyazovskaya, S. V. Eremeev, A. Ernst, P. M. Echenique, A. Arnau, and E. V. Chulkov, Phys. Rev. Lett. **122**, 107202 (2019).
14. A. M. Shikin, D. A. Estyunin, D. A. Glazkova, S. O. Fil'nov, and I. I. Klimovskikh, JETP Lett. **115**, 213 (2022).
15. S. A. Altshuler and B. M. Kozyrev, *Electron Paramagnetic Resonance in Compounds of Transition Elements* (Wiley, New York, 1974; Nauka, Moscow, 1972).
16. K. W. H. Stewens, Proc. Phys. Soc. A **65**, 209 (1952).

17. C. J. Ballhauzen, *Introduction to Ligand Field Theory* (McGraw-Hill, New York, 1962).
18. J. Hubbard, Proc. R. Soc. A **276**, 238 (1963).
19. B. A. Bernevig, T. L. Hughes, and S.-C. Zhang, Science (Washington, DC, U. S.) **314**, 1757 (2006).
20. X. Dang, J. D. Burton, A. Kalitsov, J. P. Velev, and E. Y. Tsymbal, Phys. Rev. B **90**, 155307 (2014).
21. V. V. Val'kov, JETP Lett. **111**, 647 (2020).
22. V. V. Val'kov, JETP Lett. **114**, 751 (2021).
23. J. Hubbard, Proc. R. Soc. A **285**, 542 (1965).
24. R. O. Zaitsev, Sov. Phys. JETP **41**, 100 (1975).
25. R. O. Zaitsev, Sov. Phys. JETP **43**, 574 (1976).
26. Y. Nagaoka, Phys. Rev. **147**, 392 (1966).
27. Yu. A. Izyumov, Sov. Phys. Usp. **34**, 935 (1991).
28. Yu. A. Izyumov, Phys. Usp. **38**, 385 (1995).
29. Yu. A. Izyumov, Phys. Usp. **40**, 445 (1997).
30. N. N. Bogolyubov, Izv. Akad. Nauk SSSR, Ser. Fiz. **6**, 77 (1947).
31. D. N. Zubarev, *Nonequilibrium Statistical Thermodynamics* (Nauka, Moscow, 1971; Springer, Berlin, 1974).
32. R. Zwanzig, Phys. Rev. **124**, 983 (1961).
33. H. Mori, Prog. Theor. Phys. **33**, 423 (1965).
34. D. J. Thouless, M. Kohmoto, M. P. Nightingale, and M. den Nijs, Phys. Rev. Lett. **49**, 405 (1982).
35. J. K. Asboth, L. Oroszlany, and A. Palyi, *A Short Course on Topological Insulators*, Lect. Notes Phys. **919**, 1 (2016).
36. V. V. Val'kov, V. A. Mitskan, A. O. Zlotnikov, M. S. Shustin, and S. V. Aksenov, JETP Lett. **110**, 140 (2019).
37. R. O. Zaitsev, J. Exp. Theor. Phys. **96**, 286 (2003).

Translated by R. Tyapaev